Combined Control of Freeway Traffic Involving Cooperative Adaptive Cruise Controlled and Human Driven Vehicles Using Feedback Control Through SUMO

Mehmet Ali Silgu, *Member, IEEE*, İsmet Gökşad Erdağı, *Member, IEEE*, Gökhan Göksu, and Hilmi Berk Celikoglu, *Senior Member, IEEE*

***Abstract*— In this study, we propose and test through micro-simulation a novel controller for the combined control of freeway traffic by adopting coordinated Ramp Metering (RM) and Variable Speed Limiting (VSL) strategies. In order to figure out the performance of the H_∞ State Feedback Controller we have designed, field observations on a real freeway segment with four on-ramps and an off-ramp in the city of Istanbul are used to calibrate the Intelligent Driver Model at SUMO (Simulation of Urban MObility). Scenarios with varying penetration rates of vehicles with Cooperative Adaptive Cruise Control (CACC) in mixed traffic are simulated through SUMO specific to the cases of no control, only coordinated RM control, and the combined coordinated RM + VSL control. Performance of the controller we have proposed has been analyzed considering a number of measures on traffic flow dynamics and emissions exhausted. We define three critical levels for penetration rates of vehicles with CACC in freeway traffic.**

***Index Terms*— Control theory, road traffic control, state feedback, robust control, autonomous vehicles, connected vehicles, cruise control, simulation.**

I. Introduction

With the increase in population, and hence the corresponding demand for transport, advances in both the vehicular and the communication technology have urged the agencies involved in traffic management to improve the efficiency in the use of roads' capacities through Intelligent Transportation Systems (ITS). Implementations of a certain number of systems, i.e., Ramp Metering (RM), Variable Speed Limits (VSL), Variable Message Signs (VMS), and route guidance, have therefore become the most widely known ITS tools. The related literature shows that it is also possible to increase the efficiency in managing road traffic by using such tools in conjunction in an integrated framework and by alternating the methods of control adopted. Furthermore, the recent advances in communications and their integration to what the recent vehicular technology suggests reinforce the effectiveness of ITS tools through Vehicle-to-Vehicle (V2V) and Vehicle-to-Infrastructure (V2I) communication channels.

Determining an optimal rate of penetration for Cooperative Adaptive Cruise Control (CACC) controlled vehicles in mixed traffic has consequently been the goal of a wide range of studies that involve traffic flow modeling and control under different setups. This emerging research direction provides significant inputs to the long-term strategies in planning the infrastructure, which the introduction of connected vehicles to actual traffic necessitates. In other words, having projection on the market penetration rates of connected vehicles and on the effectiveness of varying penetration rates helps to minimize in short-term the costly investments for the required infrastructure by spreading over long term. Therefore, our motivation in the present study has been to improve the performance of the control we apply on mixed traffic flow, which is composed of Human Driven Vehicles (HDVs) and CACC equipped vehicles. Towards our motivation, we propose theoretically a complete control system for freeway networks by combining the RM and VSL tools, while we reveal using real data the performance of the controller that we have introduced for the first time in the literature to the integrated management of freeway traffic.

In order to maintain the robustness in the presence of disturbances, which may yield to poor performance of the system behavior in the existence of exogeneous inputs, we have made use of an H_∞-based control strategy. One of the major advantages of such a control strategy is that, it can be guaranteed that the dynamical system evolves properly in the absence of disturbances and such a nominal behavior is preserved up to a steady-state error proportionally with the applied disturbance and an H_∞ gain in the presence of

Manuscript received 3 August 2020; revised 19 March 2021; accepted 16 July 2021. Date of publication 3 August 2021; date of current version 9 August 2022. This work was supported in part by the Scientific and Technological Research Council of Turkey (TUBITAK) under Project 120M576. The Associate Editor for this article was G. Ostermayer. *(Corresponding author: Hilmi Berk Celikoglu.)*

Mehmet Ali Silgu is with the ITU ITS Research Laboratory, Istanbul Technical University (ITU), 34469 Istanbul, Turkey, and also with the Department of Civil Engineering, Bartın University, 74100 Bartın, Turkey (e-mail: msilgu@itu.edu.tr).

İsmet Gökşad Erdağı and Hilmi Berk Celikoglu are with the ITU ITS Research Laboratory, Istanbul Technical University (ITU), 34469 Istanbul, Turkey, and also with the Department of Civil Engineering, Istanbul Technical University (ITU), 34469 Istanbul, Turkey (e-mail: erdagi@itu.edu.tr; celikoglu@itu.edu.tr).

Gökhan Göksu is with the ITU ITS Research Laboratory, Istanbul Technical University (ITU), 34469 Istanbul, Turkey (e-mail: goksug@itu.edu.tr).

Digital Object Identifier 10.1109/TITS.2021.3098640

perturbations. In this study, we incorporate the H_∞ State Feedback Controller into the integrated management system of freeway traffic in order to sustain the mainstream traffic under a critical density by considering the queue lengths on on-ramps and the downstream and upstream occupancies on the mainstream in the presence of disturbances resulting from the inflows coming to the mainstream and from the on-ramps.

On the contrary to other robust control strategies, H_∞-based control is generally adopted when using linear models. However, this does not affect the case we consider as the traffic flow model that we use is linear in terms of the density and the queue lengths at on-ramps. In order to formulate the flow of traffic, we adopt the ordinary differential equations (ODE) model of Lighthill-Whitham-Richards (LWR) (see Chapter 9 of [1]). The analyses involving the integrated control have been conducted over the micro-simulation environment SUMO (Simulation of Urban MObility) using the characteristics of a real network and the model parameters calibrated according to the field data. The novelty in the present study is three-folds:

- Proposing an integrated RM and VSL scheme by using an H_∞ State Feedback Controller;
- Performing the integrated control for freeway traffic through RM and VSL making use of real data; and,
- Discussing the effects of the combined control with the H_∞ State Feedback Controller on the penetration rates of CACC equipped vehicles in mixed traffic.

The notation in this paper is fairly standard. "*" represents the conjugate block of the upper triangular matrix. All the matrices are assumed to have compatible dimensions for algebraic operations. For vectors $\mathbf{x}$ and $\mathbf{y}$, and a positive definite symmetric matrix P, $\mathbf{x}^T P\mathbf{y}+\mathbf{y}^T P\mathbf{x}$ is written in short as $2\mathbf{x}^T P\mathbf{y}$.

We organize the rest of the article as follows: In the following section, we present a comprehensive literature review on freeway traffic control strategies and the CACC. We introduce the description and the formulation of the control problem, together with the definition of the H_∞ State Feedback Controller, in Section III. In Section IV, we introduce the micro-simulation model we have developed at SUMO and, its calibration and validation using field data. We discuss the results from solutions in Section V, and conclude the article with our findings and the future research directions in the final section.

II. Literature Review

In addition to the fact that the application of RM and VSL tools have been extensively studied through the years, the adaptation of communication technologies to vehicles has increased the performance of control on traffic flow even further. In this context, we therefore discuss in the following the benefits and limitations of freeway control strategies and connected and autonomous vehicles (CAVs) from the experiences that we have learnt through the studies.

Haj-Salem and Papageorgiou ([2]) presented their field results that are obtained from RM application based on the feedback control strategy, ALINEA. Although their results were found to be promising, the unfamiliarity of drivers to such kind of applications is mentioned as an obstacle for further improvements. In [3], an optimal control based RM strategy is adopted in order to minimize Total Time Spent (TTS), through a control problem involving the LWR traffic flow model. Having achieved reduction in the TTS on both the mainstream and the on-ramp, the need to activate the RM controller simultaneously with the shift of the traffic state to congestion is stressed. Zhang and Ritchie ([4]) have tried to improve the performance of RM strategies by alternatively employing Artificial Neural Networks (ANN) through non-linear feedback control.

Adopting a Linear Quadratic (LQ) control approach, Zhang *et al.* ([5]) have tested a coordinated ramp control algorithm by alternating the demand of on-ramp flows together with the mainstream capacities, where decreases in both the travel and the queuing time have been achieved over the mainstream and the on-ramps. Smaragdis *et al.* ([6]) have proposed a variant of the feedback controller ALINEA in order to increase controller's performance in changing traffic conditions. The performance of the controller proposed is tested with no downstream measurements as well in [6]. In our opinion, the significant finding in [6] is the use of changing the critical density, which helps to decide the activation of the RM controller. Based on field observations at an isolated freeway segment with merging flows, Cassidy and Rudjanakanoknad ([7]) have argued that an RM strategy should consider mostly the characteristics of shoulder lane and the traffic it accommodates. Thus, it is understood that the macroscopic model-based simulations can present exaggerated results. Gomes and Horowitz ([8]) have widened the range of applied flow models for setting up RM strategies by introducing feasible conditions to use the Asymmetric Cell Transmission Model (ACTM). Hou *et al.* ([9]) have adopted the iterative learning control approach as an add-on to an existing feedback control algorithm in order to overcome the drawbacks that exist due to the uncertainty in traffic flow. In addition, feasible conditions to employ Iterative Learning Control (ILC) for a density control problem formulated using the LWR model is shown in [9]. Gomes *et al.* ([10]) have performed a complete theoretical analysis of using the Cell Transmission Model (CTM) for an RM strategy, in which equilibrium points for different cases have been obtained. It is further argued in [10] that even in cases with excessive demand, the RM can prevent potential congestions, which signifies that finding an appropriate activation point for the RM should not be considered as an issue. Underlining that the ramp capacity possesses a significant limitation for the performance of their approach, Papamichail *et al.* ([11]) have developed a rolling-horizon hierarchical coordinated control system, which updates the solution for defined control horizons. In order to deal with the on-ramp capacity problem more realistically, Haddad *et al.* ([12]) have handled both urban and freeway networks and, have employed the Macroscopic Fundamental Diagram (MFD) representation for two urban networks and the ACTM for a freeway network. The interflows between two urban networks and the inflows to the freeway are regulated

with a Model Predictive Control (MPC) scheme, in which: for higher performances the need to centralized control; and, for increasing the efficiency improvements in the route choice modeling are stressed.

Studies summarized above focus mainly on improving selected performance(s), especially in terms of TTS, and/or maintaining the flow of the traffic around a critical density. Pasquale *et al.* ([13]) have advanced the RM research by seeking the optimal solution for the control problem involving the minimization of two objectives, i.e., the TTS and total emissions. Despite the fact that a more realistic composition of traffic involving two vehicle classes, i.e., passenger-car and truck, is considered in [13], the average speed based calculation of pollutants through the emission model adopted overshades the contribution of having introduced different vehicles classes to the problem formulation. However, the approach in ([13]) is a significant advance in considering environmental factors. In conjunction with the findings in [13] that stress the need of a control strategy to satisfactorily perform under varying conditions, Kan *et al.* ([14]) have investigated the effectiveness of both the ALINEA and the PI-ALINEA controllers for different road characteristics, where the geometry of the road that accommodates the mainstream involves lane-drops. Corroborating the findings from simulation by field experiments, Kan *et al.* ([14]) have shown that the ALINEA is more sensitive to the changes in conditions than the PI-ALINEA.

It is straight to conclude that freeway flow control using a singular strategy, such as in the case of above mentioned works involving solely RM or as discussed in [15] regarding VSL, without any combination has drawbacks when compared to combined control, i.e., RM and route guidance ([16]–[18]), VSL and lane control ([19]), and RM with VSL, as reviewed in the following.

Hegyi *et al.* ([20]) have adopted an MPC framework in order to optmize the system perfomance aiming to minimize the TTS through RM and VSL. Using METANET to model the traffic flow, an interesting comparison between the mainstream control performances of VSL and lane-based mainstream metering is presented in [20], where the mainstream metering has been found to be triggering oscillations, and hence shockwaves, on traffic flow. In order to figure out the performance of combined management approach, which involves RM, VSL, and route guidance, through an optimal control formulation using a real-world freeway network, Carlson *et al.* ([21]) have utilized the METANET model, as well and, have highlighted the need to reinforce RM applications with other tools. Frejo and Camacho ([22]) have improved the use of MPC for RM and VSL in order to present a comparison between the algorithms of MPC through local, centralized, and decentralized systems. It is found in [22] that although the implementation of a centralized system is an issue, the centralized control performs better. Carlson *et al.* ([23]) have proposed a feedback control based combined system of RM and VSL, where the two activation points of VSL are set to be the times that the RM component suggests an inapplicable metering rate and the capacity of the ramp is forced to be exceeded. Though the integrated system is found to perform better, the need to define properly the control period of each system for better performances is highlighted ([23]). Using a discrete speed limit approach through MPC, Frejo *et al.* ([24]) have proposed a combined RM and VSL system and, highlighted the need to trade-off between the accuracy and the computation time. Zhang and Ioannou ([19]) proposed an integrated system of RM and VSL with the addition of lane change control, where the ALINEA-Q and a VSL algorithm are employed to maximize the throughput of the system and to figure out as well the changes in emissions by simulation modeling through VISSIM.

As in conjunction with the advances in vehicular and communication technology, and hence the increasing interest in autonomous systems, the recent research trend on road traffic control concentrates on the performance of CAVs in either mixed traffic flow or a complete autonomous traffic system. In this context, Roncoli *et al.* ([25]) have sought the optimal solution for an integrated system consisting of RM, VSL and lane change control, in which mixed traffic composition by HDVs and CAVs is considered. Roncoli *et al.* ([26]) have further utilized the MPC approach for a freeway control problem similar to the one in [25], where they have investigated as well the effect of three levels of varying penetration rates of CAVs in mixed traffic.

Analyses on the effects of varying penetration rates have been reported in most of the recent related studies in order to evaluate in terms of safety, environmental effects, and flow dynamics the performance of the controlled system involving CAVs. As one of the earliest studies, Ioannou and Chien ([27]) have pointed out the potential benefits as organizing traffic flow and improving traffic safety, which have then become the two major directions for analyzing the effects of CAVs. At this point, vehicle motion control exists as a significant research area. Involving several control objectives related to safety, comfort, and efficiency, Wang *et al.* ([28]) have made use of dynamic programming. HomChaudhuri *et al.* ([29]) have focused mainly on the fuel efficiency. An MPC algorithm to minimize fuel consumption, and the variations on speed and spacing is proposed in [29]. Zhou *et al.* ([30]) have proposed a rolling horizon stochastic optimal control strategy to maintain a constant headway between vehicles, in which the effects of measurement errors of the systems are aimed to be reduced. Milanes and Shladover ([31]) have developed a car-following model, in which the maintenance of constant time headways between vehicles is sought. The algorithm proposed in [31] is shown to perform better in damping the existing speed oscillations in comparison to an adaptive cruise control algorithm that is used in conjunction with a widely used car-following model, the Intelligent Driver Model. Milanes and Shladover ([31]) have shown that the algorithm they propose is suitable for real-world applications and can be used as a car-following model in simulation environments, as well. Li *et al.* ([32]) have considered mixed traffic composition of HDVs and CAVs to propose an appropriate VSL algorithm for CAVs. In order to increase the human effect in traffic flow, the compliance rate of drivers is decreased in [32], where the adoption of such kind of applications is recommended for the early development stages of CAVs.

As documented in the below summarized literature, a CACC model should satisfy several driving goals safely and efficiently, in addition to the fact that it has to provide string stability and traffic flow stability. Talebpour and Mahmassani ([33]) and Lee *et al.* ([34]) have presented extensive stability analyses involving CAVs. Xiao *et al.* ([35]) have considered activation/deactivation of the control system on stability and, Tu *et al.* ([36]) have conducted a similar analysis in terms of traffic safety. In [36], using the CACC model proposed in [31], the variation of surrogate safety measures, i.e., time-to-collision, total time spent under dangerous traffic conditions, and time integrated time-to-collision, is figured out. Li *et al.* ([37], [38]) have provided a detailed safety analysis on CACC with the consideration of different weather conditions, different intelligent safety systems, and freeway control strategies through the surrogate safety measures considered in [38].

The effects of the variation on the penetration rates of CAVs in traffic flow have been extensively studied. Van Arem *et al.* ([39]) have discussed the potential capacity improvement with varying penetration rates of CACC equipped vehicles, where they have indicated that lower than 40% penetration rate would not have any effect on traffic flow performance, but 60% would. Zhao and Sun ([40]) have presented a simulation framework for modeling and analyzing CACC based car-following models and platoons, where they have achieved a capacity increase at each penetration rate, in contrast to [39]. Knorr *et al.* ([41]) have focused on the shockwave mitigation effect of CAVs and, figured out that after the 30% of penetration rate, the improvements would be apparent. Delis *et al.* ([42]) have adopted a macroscopic approach to analyze the varying penetration rates of CACC equipped vehicles on density evolution on-road segments. The 30% of penetration rate has been found to be an indicative level, as well in [42]. Liu *et al.* ([43]) have conducted a broader analysis in order to find the critical levels for penetration rates. Vehicle Awareness Device (VAD) equipped vehicles are considered in the traffic composition in order to increase the probability of forming platoons ([43]). The results in [43] have shown that, although 100% of penetration rate can nearly double the capacity, for the penetration rates lower than 60% the improvements achieved are minor.

In summary, methodologically, optimal control and feedback control approaches comprise a significant part of the literature on freeway traffic control. The review on related literature shows that the performance of the H_∞ state feedback control approach has not been investigated in freeway traffic management involving combined control strategies and mixed traffic with CAVs. Our contributions to the related literature are therefore as follows:

- Proposing an integrated RM and VSL control approach with a powerful robust control tool using H_∞ theory;
- Discussing the compatibility of CACC with an existing ITS application without V2I communication;
- Figuring out the potential improvements provided by our novel approach based on H_∞ state feedback control; and,
- Discussing the indicative levels for penetration rate in terms of traffic flow performance and emissions.

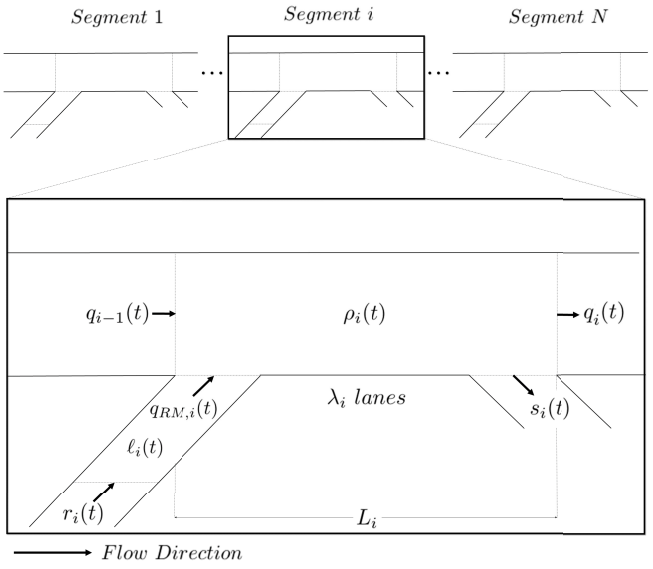

Fig. 1. The generic freeway.

TABLE I
THE DESCRIPTION OF VARIABLES PRESENTED IN FIGURE 1

Variable	Description
$\rho_i(t)$	Density on Segment i of road at time t
$q_i(t)$	Number of vehicles coming from the road Segment i into the road Segment $i+1$ at time t
$\ell_i(t)$	Queue length of the ramp entering into the Segment i at time t
$q_{RM,i}(t)$	Number of vehicles entering from the on-ramp into Segment i at time t
$s_i(t)$	Number of vehicles leaving from the Segment i to join the off-ramp at time t
$r_i(t)$	Number of vehicles entering the i^{th} on-ramp at time t

III. PROBLEM STATEMENT

A. Ramp Metering and Variable Speed Limit Setting

In this study, we consider the integrated RM and VSL control problem on a freeway with multiple on-ramps and multiple off-ramps as depicted in Fig. 1, where the variables shown are described in Table I.

Concerning the mainstream dynamics schematically represented in Fig. 1, we obtain the following systems of differential equations, for all $i = 1, 2, \ldots, N$ as:

$$\dot{\rho}_i(t) = \frac{q_{i-1}(t) + \delta_{r,i} q_{RM,i}(t) - q_i(t) - \delta_{s,i} s_i(t)}{\lambda_i L_i}, \qquad (1)$$

where L_i is the length and λ_i is the number of lanes of the Section i. In order to reflect the network topology, we also define $\delta_{r,i}$ and $\delta_{s,i}$, the on-ramp and off-ramp indicators, indicating that there is an on-ramp and/or off-ramp on the segment i. $\delta_{r,i} = 1$ ($\delta_{s,i} = 1$) implies that there exists an on-ramp (off-ramp, respectively) whereas $\delta_{r,i} = 0$ ($\delta_{s,i} = 0$) implies that there is no on-ramp (off-ramp, respectively) on the Segment i.

Following the ramp dynamics shown by Fig. 1, the flow conservation throughout the stretch we consider can be written

as:

$$\dot{\ell}_i(t) = r_i(t) - q_{RM,i}(t), \quad \text{for } i = 1, 2, \ldots, N. \tag{2}$$

The macroscopic fundamental diagram of Flow vs. Density we adopt is derived from the microscopic theory (see [44]) as a piecewise function that is defined in part specific to the traffic states of free-flow and congested flow:

$$q(\rho) = \begin{cases} v_f \rho, & \rho < \rho_c \\ C\left(1 - \dfrac{\rho}{\rho_{max}}\right), & \rho \geq \rho_c \end{cases}$$

Here, v_f is the free-flow speed, ρ_c is the critical density, ρ_{max} is the maximum density, and C is a sensitivity parameter. Defining the error term $e_i(t)$ as $e_i(t) = \rho_i(t) - \rho_c$, for $i = 1, 2, \ldots, N$, yields to the following flow dynamics for the congested state given as:

$$q_i(t) + \delta_{s,i} s_i(t) = C\left(1 - \frac{e_i(t) + \rho_c}{\rho_{max}}\right). \tag{3}$$

Thus, the error dynamics can be written for the Segment 1 as:

$$\dot{e}_1(t) = \frac{C}{\rho_{max}\lambda_1 L_1} e_1(t) + \frac{\delta_{r,1}}{\lambda_1 L_1} q_{RM,1}(t) + \frac{1}{\lambda_1 L_1} q_0(t) - \frac{C}{\lambda_1 L_1}\left(1 - \frac{\rho_c}{\rho_{max}}\right), \tag{4}$$

and, for Segments $i = 2, \ldots, N$, as:

$$\dot{e}_i(t) = \frac{C}{\rho_{max}\lambda_i L_i} e_i(t) - \frac{C}{\rho_{max}\lambda_i L_i} e_{i-1}(t) + \frac{\delta_{r,i}}{\lambda_i L_i} q_{RM,i}(t) - \frac{\delta_{s,i}}{\lambda_i L_i} s_{i-1}(t). \tag{5}$$

Defining the state vector

$$\mathbf{x}(t) = \begin{bmatrix} e_1(t) & e_2(t) & \cdots & e_N(t)\ell_1(t) & \ell_2(t) & \cdots & \ell_N(t) \end{bmatrix}^\top, \tag{6}$$

the control vector

$$\mathbf{u}(t) = \begin{bmatrix} u_{VSL}(t) & u_{RM,1}(t) & u_{RM,2}(t) & \cdots & u_{RM,N}(t) \end{bmatrix}^\top, \tag{7}$$

with its components

$$u_{VSL}(t) = q_0(t) - C\left(1 - \frac{\rho_c}{\rho_{max}}\right),$$
$$u_{RM,i}(t) = q_{RM,i}(t), \quad \text{for } i = 1, 2, \ldots, N, \tag{8}$$

the disturbance vector

$$\mathbf{w}(t) = \begin{bmatrix} s_1(t) & s_2(t) & \cdots & s_{N-1}(t)r_1(t) & r_2(t) & \cdots & r_N(t) \end{bmatrix}^\top, \tag{9}$$

and writing (4)-(5) with (2) in a compact form yields:

$$\dot{\mathbf{x}}(t) = \mathbf{A}\mathbf{x}(t) + \mathbf{B_u}\mathbf{u}(t) + \mathbf{B_w}\mathbf{w}(t), \tag{10}$$

where

$$\mathbf{A} = \left[\begin{array}{c|c} \overline{\mathbf{A}} & \mathbf{0}_{N\times N} \\ \hline \mathbf{0}_{N\times N} & \mathbf{0}_{N\times N} \end{array}\right], \tag{11}$$

$$\mathbf{B_u} = \left[\begin{array}{c|c} \overline{\mathbf{B}} & \overline{\mathbf{B}}_\mathbf{u} \\ \hline \mathbf{0}_{N\times 1} & -\mathbf{I}_N \end{array}\right] \tag{12}$$

$$\mathbf{B_w} = \left[\begin{array}{c|c} \overline{\mathbf{B}}_\mathbf{w} & \mathbf{0}_{N-1\times N} \\ \hline \mathbf{0}_{N\times N-1} & -\mathbf{I}_N \end{array}\right]. \tag{13}$$

with

$$\overline{\mathbf{A}} = \begin{bmatrix} \dfrac{C}{\rho_{max}\lambda_1 L_1} & 0 & \cdots & 0 \\ -\dfrac{C}{\rho_{max}\lambda_2 L_2} & \dfrac{C}{\rho_{max}\lambda_2 L_2} & \cdots & 0 \\ \vdots & \vdots & \ddots & \vdots \\ 0 & 0 & \cdots & \dfrac{C}{\rho_{max}\lambda_N L_N} \end{bmatrix}, \tag{14}$$

$$\overline{\mathbf{B}}_\mathbf{u} = \text{diag}\left\{\frac{\delta_{r,1}}{\lambda_1 L_1}, \frac{\delta_{r,2}}{\lambda_2 L_2}, \cdots, \frac{\delta_{r,N}}{\lambda_N L_N}\right\}, \tag{15}$$

$$\overline{\mathbf{B}} = \begin{bmatrix} \dfrac{1}{\lambda_1 L_1} & 0 & \cdots & 0 \end{bmatrix}^\top, \tag{16}$$

$$\overline{\mathbf{B}}_\mathbf{w} = \begin{bmatrix} -\dfrac{\delta_{s,1}}{\lambda_2 L_2} & 0 & \cdots & 0 \\ 0 & -\dfrac{\delta_{s,2}}{\lambda_3 L_3} & \cdots & 0 \\ \vdots & \vdots & \ddots & \vdots \\ 0 & 0 & \cdots & -\dfrac{\delta_{s,N-1}}{\lambda_N L_N} \end{bmatrix}. \tag{17}$$

B. H_∞ State Feedback Controller

In this subsection, we design the H_∞ State Feedback Controller for the closed-loop system (10). We define the state feedback controller as:

$$\mathbf{u}(t) = \mathbf{K}\mathbf{x}(t), \tag{18}$$

and, hence, the corresponding closed-loop system (CLS) is:

$$\dot{\mathbf{x}}(t) = \mathbf{A_K}\mathbf{x}(t) + \mathbf{B_w}\mathbf{w}(t) \tag{19}$$

where $\mathbf{A_K} = \mathbf{A} + \mathbf{B_u}\mathbf{K}$.

In the following, we define the H_∞ State Feedback Controller for coordinated RM and VSL strategies.

Definition 1: Given a scalar $\gamma > 0$. The state feedback controller (18) *is said to be an H_∞ controller for* (10)*, if the following two conditions hold*:

- *The CLS* (19) *is asymptotically stable with zero disturbance input* $\mathbf{w}$.
- *Under zero initial condition, there exists a continuously differentiable Lyapunov function $V : \mathbb{R}^n \to \mathbb{R}_{\geq 0}$ satisfying $\dot{V}(t) < \gamma^2 \mathbf{w}^T(t)\mathbf{w}(t) - \mathbf{x}^T(t)\mathbf{x}(t)$ along the solutions of* (19) *for every square integrable disturbance* $\mathbf{w}$ *on* $[0, \infty)$.

Theorem 1: The state feedback controller (18) *is said to be an H_∞ controller for given $\gamma > 0$, if there exists matrices $\mathbf{P} > 0$ and $\mathbf{Y}$ satisfying*

$$\begin{bmatrix} \Omega_{11} & \mathbf{B_w} & \mathbf{P} \\ * & -\gamma^2\mathbf{I} & 0 \\ * & * & -\mathbf{I} \end{bmatrix} < 0. \tag{20}$$

where $\Omega_{11} = \mathbf{A}\mathbf{P} + \mathbf{P}\mathbf{A}^T + \mathbf{B_u}\mathbf{Y} + \mathbf{Y}^T\mathbf{B_u}^T$. The gain matrix is perceived as $\mathbf{K} = \mathbf{Y}\mathbf{P}^{-1}$.

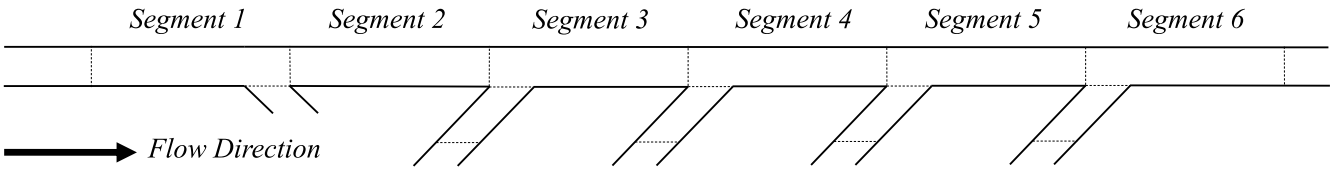

Fig. 2. Schematic representation of test stretch over E-80 freeway.

IV. Methodology and Simulation

In the following, we first introduce the microsimulation environment we utilize preceding the calibration procedure we have followed. Then, information on calibrated parameters of both the car-following and the lane-change models adopted for CACC and HDVs are provided. In order to discuss the environmental effects of controls applied, HBEFA emission model employed is briefly explained. The setting up of the strategies that are combined in the integrated control and, the SUMO simulation setup are presented finally preceding the performance measures that are defined to evaluate the controls applied.

A. Microsimulation Environment: Eclipse SUMO

The Eclipse SUMO (Simulation of Urban Mobility), an open-source microscopic traffic simulation software developed by the German Aerospace Center (DLR), is utilized as the simulation environment. In SUMO, there are several internal tools, including NETCOVERT, NETEDIT, TRACI, for modeling networks and traffic demands. In the present study, the layout of the freeway network is extracted from OpenStreetMap and, then converted into a readable format for Eclipse SUMO via NETCONVERT. Then, the corrections for acceleration and deceleration lanes, control strategies at on-ramps, and lengths of on-ramps and off-ramps are applied through NETEDIT. Traffic demands are coded via a code editor software in a readable format for Eclipse SUMO. Finally, the proposed control strategy is coded in Python language, which is the appropriate format for TRACI. TRACI is used for connecting and intervening simulation at the predetermined simulation steps.

B. Freeway Network and Calibration Process

The freeway network we consider is a piece of the E-80 Freeway in Istanbul. The modeled stretch of the freeway consists of four on-ramps and an off-ramp. The characteristics of the freeway stretch that is schematically shown in Fig. 2 are presented in Table II.

The field data is obtained by the microwave sensor units, four of which are located at the sections downstream the merges of on-ramps, and the fifth sensor is located on the mainline upstream the diverge of the off-ramp.

The car-following model for human drivers follows the Intelligent Driver Model ([45]), further information on which is given in Section V-C. While calibrating the model, the difference between the measured traffic flows and the simulated traffic flows are sought to be minimized. Following [46] and [47], the GEH Statistics and Theil's Coefficients are selected as the measures considered in calibration. GEH Statistics is defined as given by (21):

TABLE II
Freeway Stretch Characteristics

Segment No	No. of Lanes	Length	Density
1	4	4.29 km	$\rho_1(t)$
2	3	0.79 km	$\rho_2(t)$
3	3	0.96 km	$\rho_3(t)$
4	4	0.67 km	$\rho_4(t)$
5	4	0.03 km	$\rho_5(t)$
6	4	1.14 km	$\rho_6(t)$

$$GEH = \sqrt{(y-x)^2/((y+x)/2)}, \tag{21}$$

where y and x represent respectively the obtained traffic flow from simulation results and the observed traffic flow through field surveys. The result from (21) corresponds to a real number, so that the way to obtain this statistics can be defined as a modified chi-square test that requires the signification of the values obtained.

In this study, the measures for GEH Statistics are considered following [48]: GEH Statistics of individual link flows must be less than 5 for 85 % of the cases; and, GEH Statistics for the sum of all link flows must be less than 4. The differences between the simulated flows and measured flows are presented in Fig. 3 and, the temporal variations of the corresponding GEH values are shown in Fig. 4. On the real network, the measurements are retrieved at points located at the end of each ramp, and at the first 1000 meters of the mainline. The simulated data are retrieved at locations matching the actual points of measurement on the real network.

As can be seen from Fig. 4, the GEH values that are calculated using network flows existed within the defined threshold ([48]) in most of the time, approximately 91.11% of time.

The other calibration measures selected are the Theil's Coefficients, as using such measures help to obtain the characteristics of the modeling error from different aspects ([46]). U_m gives the measure of bias between the data sets of observations and simulation, where a value between 0 and 0.1 is acceptable ([47]).

The U_m is obtained using (22):

$$U_m = \frac{n(\bar{y}-\bar{x})^2}{\sum_{i=1}^{n}(y_i - x_i)^2}, \tag{22}$$

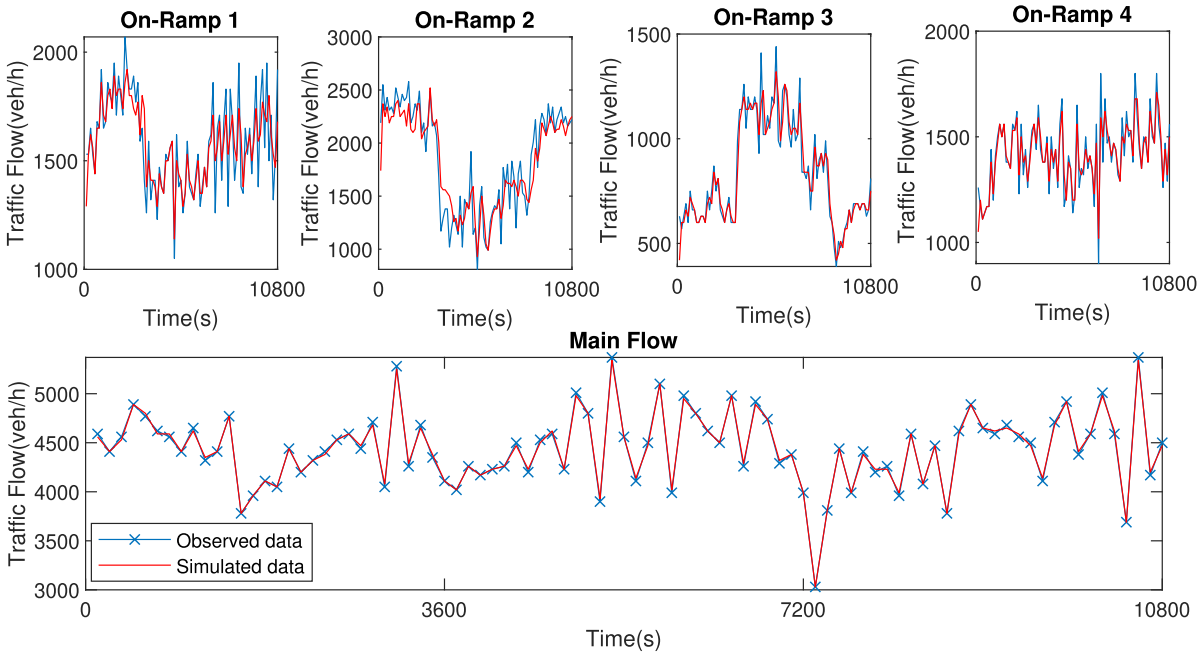

Fig. 3. Traffic flow profiles through calibration: observed vs. simulated.

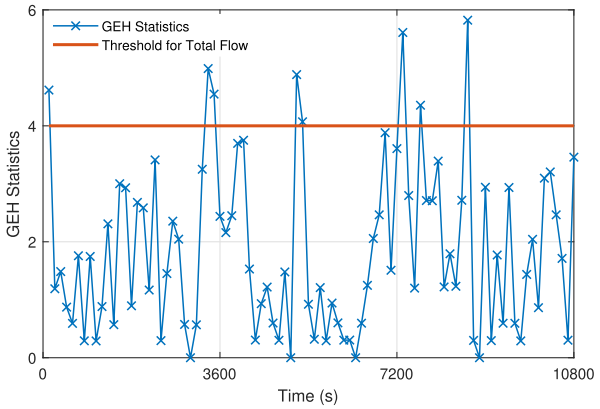

Fig. 4. Variation of GEH statistics obtained through calibration.

where n, $\bar{y}$, $\bar{x}$, y_i, and x_i represent respectively the number of observations, mean of simulated quantities, mean of observations, ith simulated quantity, and ith observation. Investigation of the similarity of fluctuations between the field data and simulated data is obtained using U_s that is calculated as in (23):

$$U_s = \frac{n(\sigma_x - \sigma_y)^2}{\sum_{i=1}^{n}(y_i - x_i)^2}, \tag{23}$$

where σ_x and σ_y represent respectively the standard deviation of simulated and observed quantities. The acceptable range of U_s is between 0 and 0.1 ([47]). The last coefficient, U_c, whose acceptable value falls within the range from 0.9 to 1.0 ([47]), is calculated as given by (24):

$$U_c = \frac{2(1-r)\sigma_x\sigma_y}{\sum_{i=1}^{n}(y_i - x_i)^2}, \tag{24}$$

TABLE III
CALIBRATION MEASURES FOR MICRO-SIMULATION MODEL: THEIL'S COEFFICIENTS

	Main Stream	On-Ramp 1	On-Ramp 2	On-Ramp 3	On-Ramp 4	Total Flow
U_m	0.001	0.004	0.015	0.002	0.003	0.016
U_s	0.168	0.129	0.051	0.013	0.170	0.015
U_c	0.830	0.865	0.932	0.983	0.825	0.968

where r represents the coefficient of correlation. Theil's coefficients that we have obtained while calibrating the micro-simulation model are presented in Table III.

C. Car-Following Models for HDVs and CACC, and Lane Change Model

For modeling the longitudinal vehicle motion that is controlled by human drivers, the Intelligent Driver Model (IDM) proposed by Treiber, Hennecke, and Helbing ([45]), which is a single-lane car-following model based on the acceleration function of vehicles, is utilized. The widely used IDM has also constituted a basis for development of two car-following models, i.e., Human Driver Model ([45]) and Enhanced Human Driver Model ([49]). Each of these models has improved the IDM in terms of reflecting the actual behavior of human drivers, however, in our case, we have utilized IDM on purpose due to the relatively lower computational performance it requires, as figured out in [49]. Using the IDM, the acceleration can be obtained as given by (25):

$$\dot{v_a} = a^{(a)}[1 - (v_a/v_0^{(a)})^{\delta} - (s^{\star}(v_a, \triangle v_a)/s_a)^2], \tag{25}$$

where $\dot{v_a}$, a, v, v_{des}, δ, $s^{\star}$, $\triangle v_a$, and s_a represent respectively the calculated acceleration, maximum acceleration, velocity, desired velocity, acceleration exponent, minimum spacing,

TABLE IV
VALUE OF PARAMETERS FOR IDM

Des. Speed (m/s)	Acceleration (m/s^2)	Deceleration (m/s^2)	δ	Headway (s)	Min. Gap
25	2	2	4	1.5	0

TABLE V
FEEDBACK GAINS ADOPTED SPECIFIC TO TRAFFIC CONDITIONS

	Speed Control Mode	Gap Closing Mode	Gap Control Mode
k_0	0.4 s^{-1}	-	-
k_p	-	0.005 s^{-1}	0.45 s^{-1}
k_d	-	0.05	0.0125

velocity difference to the leading vehicle, and spacing. Since the vehicle length affects the spacing between vehicles, it is considered as a parameter for calibration. Having calibrated the model at SUMO, the model parameters obtained are given in Table IV. While modeling the traffic with CAVs, several assumptions are made as listed in the following: i) Each of the vehicles in the traffic flow has a VAD, therefore, even if a vehicle is not equipped with the CACC system, it transmits its speed and location; ii) There is no merging assistance for vehicles, therefore, drivers have to turn off the CACC system and make a lane change maneuver after they complete the lane change maneuver and, the system is activated again; and, iii) There is no time loss between the activation and deactivation process. Adhering the assumptions made, it is fair to model CACC as a car-following model. In this study, we have utilized the CACC based car-following model in SUMO, which is proposed by Milanes and Shladover ([31]). In this model, car-following behavior is modeled in three conditions, i.e., speed control mode, gap closing mode, and gap control mode. In speed control mode, when the time headway is greater than 2 s, the difference between the desired speed and the actual speed is controlled by acceleration as given by (26).

$$a_k = k_0(v_{des} - v_{k-1}), \tag{26}$$

Furthermore, car-following behavior is modeled as a function of error terms and two feedback gains: for gap control mode, when the spacing between vehicles is less than 0.2 m, and speed deviation between vehicles are 0.1 m/s, and for gap-closing mode, when the time headway is less than 1.5 s. If the headway is in between 1.5 s and 2 s, the vehicles keep their ultimate control mode. Here, the speed in ultimate control mode is calculated as in (27):

$$v_k = v_{k_{prev}} + k_p e_k + k_d \dot{e_k}, \tag{27}$$

where v_k, $v_{k_{prev}}$, e_k, and $\dot{e_k}$ represent respectively the speed of k^{th} vehicle, the speed of the k^{th} vehicle at the previous time step, the bias from the desired spacing between k^{th} and $(k-1)^{th}$ vehicles, and the first-order derivative of the error term. The error term is is obtained by (28):

$$e_k = x_{k-1} - x_k - t_{hw} v_k, \tag{28}$$

where x_{k-1}, x_k, and t_{hw} represent respectively the location of the $(k-1)^{th}$ vehicle, the location of the k^{th} vehicle, and the time headway. The feedback gains vary with the changing traffic conditions. The feedback gains specific to traffic conditions are adopted considering the widely used values in the literature ([31], [35], [50]) and presented in Table V.

The default lane change model in SUMO is LC2013, which is developed in [51]. In this model, four types of lane changing maneuvers, i.e., strategic change, cooperative change, tactical change, and regulatory change, are defined. In order to realistically model actual traffic flow conditions, several modifications are applied. Specifically, the eagerness for following the obligation to keep right lane is reduced, and the eagerness for performing lane change to gain speed is increased. With the selected combination of the lane change model parameters, the problem of the congestion occurence only on the rightmost lane on the mainstream is avoided.

D. Emission Model

In order to figure out the environmental impact of the integrated control we propose, the HBEFA3 emission model is utilized. Throughout the simulation of the considered network, all the vehicles' engine and exhaust features are assumed to comply with the classification of passenger cars with internal combustion engine in the HBEFA3 database. Considering the car-ownership statistics for the city that the field data of the case network is collected, all the vehicles in the traffic are assumed to be manufactured after the year 2006, and hence follow the Euro norm 4. For a fair comparison, the vehicles with CACC are assumed to follow Euro norm 4, as well. The emission model is processed by extracting data from HBEFA 3 database and, by fitting the extracted data using a continuous function, which is obtained by simplifying the function of the tractive effort that is to be produced to overcome the resistive forces against motion as given by (29):

$$c_0 + c_1 va + c_2 va^2 + c_3 v + c_4 v^2 + c_5 v^3, \tag{29}$$

where c_n, v, and a represent respectively the linear model estimation coefficients, speed, and acceleration. The coefficients of the emission function given by (29) are calibrated using the linear model estimation of Python's "statsmodels" package. The candidate functions are evaluated based on the statistical performance measures of root mean square (RMS) and t-value, and, the best fit is selected by SUMO.

E. Combined Control Applied Involving Coordinated Ramp Metering and Variable Speed Limit

In order to integrate the H_∞ SFC to SUMO, we have utilized MATLAB, Python, and TRACI. Firstly, the feedback gain matrix is obtained as $\mathbf{K} = \mathbf{YP}^{-1}$ using the LMI Solver Toolbox of MATLAB. Then, the TRACI functions for collecting real time measurements are defined in a Python script according to the layout of the road network. Finally, the H_∞ SFC integration is provided in the same Python script with the addition of the calculated feedback gain matrix K. TRACI provides a bidirectional communication between the Python script and SUMO, and hence enables to manage the on-going

simulation according to the calculated signal times and speed limits that are input from the Python script. The critical parameters of traffic flow have been set as: $v_f = 120\ km/h$, $\rho_c = 80\ veh/km/lane$, and $\rho_{max} = 200\ veh/km/lane$. The cycle time and minimum green time have been set respectively to 15 s and 5 s for ramp controls. In order to apply Theorem 1, we choose the H_∞ gain as $\gamma = 1.5$. The sensitivity constant is defined as:

$$C = \frac{v_f}{\frac{1}{\rho_c} - \frac{1}{\rho_{max}}}.$$

At the end of each cycle, the green time for the next cycle is evaluated by calculating $u_{RM,i}(k)$ for each cycle k using (8). Then the green time $GT_i(k)$ is determined from:

$$GT_i(k) = \begin{cases} MGT, & u_{RM,i}(k) < MFR \\ \dfrac{u_{RM,i}(k)}{u_{sat}} \cdot CT, & MFR \le u_{RM,i}(k) \le u_{sat}, \\ CT, & u_{RM,i}(k) > u_{sat} \end{cases}$$

where:

- MGT is the minimum green time;
- $MFR = \frac{u_{sat} \cdot MGT}{CT}$ is the minimum flow;
- CT is the cycle time; and,
- u_{sat} is the saturated flow.

In order to prevent the in-existence of green times in cases of highly congested traffic states, and hence the blockage of ramps, the minimum green time is defined to set a lower limit, where the cycle time corresponds to the upper limit. Within the limits defined, GT_i takes the calculated green time by being rounded to closest greater integer. For example, if the green time is calculated as 6.4 seconds, the green time to be flushed will be 7 seconds. In order to apply the VSL, the desired values of flow, $u_{VSL}(k)$, are calculated for each cycle k. Then $u_{VSL}(k)$ is converted to the desired speed value, $v_{VSL}(k)$, by using the speed-flow relationship of the car-following model. The speed limits to be posted, $v_{refl}(k)$, are calculated as:

$$v_{refl}(k) = \begin{cases} v_{min}, & v_{VSL}(k) < v_{min} \\ 10 \cdot \lfloor v_{VSL}(k)/10 \rfloor, & v_{min} \le v_{VSL}(k) \le v_{max}, \\ v_{max}, & v_{VSL}(k) > v_{max} \end{cases}$$

where $\lfloor \cdot \rfloor$ rounds its argument to the closest integer, $v_{min} = 50\ km/h$ is the minimum speed to be posted, and $v_{max} = 120\ km/h$ is the maximum speed to be posted. As in the same way in determining the green time in each cycle, the speed values to be posted are also defined through a piecewise function. If $v_{VSL}(k)$ falls in the range between the predetermined minimum and maximum speed values to be posted, then it is floored to the closest product of 10. For example, in case that $v_{VSL}(k)$ is calculated as 67 km/h, the speed limit $v_{refl}(k)$ will be 60 km/h.

F. Experimental Setup

The network shown by Fig. 2 is modeled using the characteristics given in Table II. The speed limit considered for the network is 120 km/h. The simulated demand profiles that are loaded at 2 minutes resolution are presented in Fig. 3. The simulation duration and the simulation step are chosen respectively as 10800 seconds and 0.1 seconds while conducting the experiments at SUMO. Each of the scenarios, i.e., no control, RM control using ALINEA, RM control using H_∞ SFC, and combined RM and VSL control using H_∞ SFC, is simulated for varying setup of market penetration rates for CACC equipped vehicles. The market penetration rates are varied as from 0 percent to 20 percent with a 1 percent increase, from 20 percent to 40 percent with a 2 percent increase, from 40 percent to 60 percent with a 4 percent increase, from 60 percent to 80 percent with a 5 percent increase, and from 80 percent to 100 percent with a 10 percent increase. As a result, effects of 42 different penetration rates are analyzed. Trials with penetration rates under 50 percent setups are conducted considering closer rates in order to observe the earlier effect of having introduced CACC equipped vehicles on traffic flow conditions.

G. Performance Measures

In order to evaluate the performance of both the overall system and the conflicting dynamics of the mainstream and the ramps, a number of performance measures including the occupancy rates on segments over the mainstream, the total system travel time, the total system throughput, the pollutants emitted, and the fuel consumption are figured out. Such measures help to evaluate the conflicting performances of ramp dynamics and the mainstream dynamics. The conflict exists due to the objective of the ramp control we apply, which is to maintain the density, and hence the occupancy, around the critical/optimal density by decreasing the occupancy in congested states that may correspond to the decrease in the total throughput of the system.

The occupancy is defined as the ratio of the total amount of time that is spent by the vehicles on the detector to the total observation time and, is calculated for the time interval i as given by (30):

$$occ_i = (t/T) \cdot 100, \tag{30}$$

where t is the time spent on the detector, and T is the total observation time. As the traffic demand is loaded to the system within the periods of 120 seconds, the observation period, T, is set to 120 seconds, as well. The detectors to retrieve data are placed 70 meters upstream from the on-ramps, however, because of the 35 meters of the segment between the third and fourth on-ramps, the detector for the corresponding segment is located at 30 meters upstream from the third on-ramp.

In order to evaluate the possible effects of the control delay, the total travel time is calculated as another performance measure. Total Travel Time is calculated as

$$\text{Total Travel Time} = \sum_{i=1}^{n} l_i / v_{harm_i}, \tag{31}$$

where n, l_i, and v_{harm_i} represent respectively the number of road segments, length of the i^{th} segment, and harmonic mean speed on the i^{th} segment.

In order to evaluate in terms of environmental sustainability the effects of the control we have designed, the exhausted

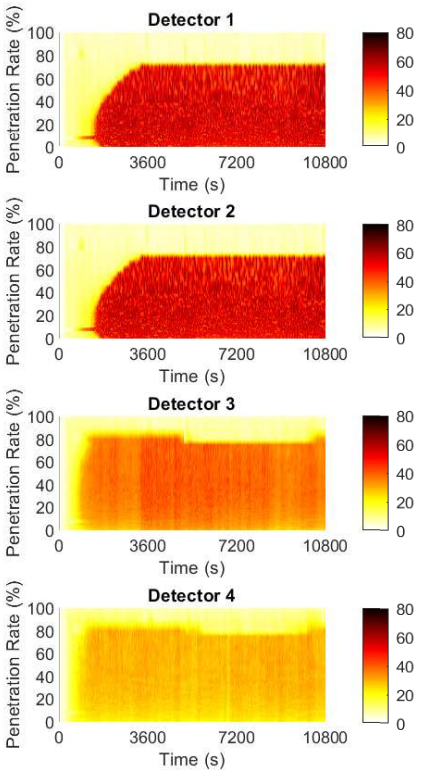

Fig. 5. Temporal variation of occupancies specific to penetration rates in no control case.

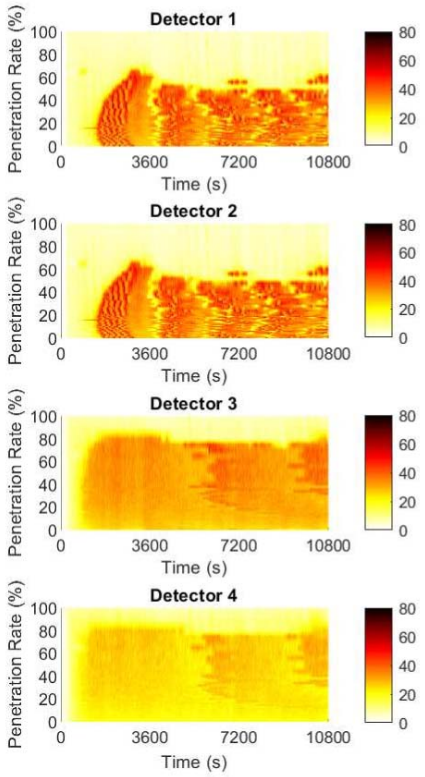

Fig. 6. Temporal variation of occupancies specific to penetration rates in case of ALINEA control.

emissions together with the fuel consumption are selected as performance measure as well. The pollutants are calculated at each time step, and aggregated over the entire duration of the simulation. The exhausted pollutants are represented in the unit of $gr/km/h$, where the unit of fuel consumption is $l/km/h$. Therefore, the dependence of the emission quantities on the length of the segment is eliminated. It is important to note that in order to figure out the harmonizing effect of the CACC equipped vehicles in the traffic flow, the trajectory data extracted is collected considering the 5 percent of the vehicles in two-seconds periods.

V. Results and Discussion

In Figs. 5 to 8, the occupancies that are retrieved by the defectors placed are shown specific to the scenarios set. The critical decreases in occupancies with penetration rates higher than 80% can be reasoned due to high harmonizing effect of CACC.

However, for a more balanced traffic composition, i.e., with around 40 to 60% of CACC equipped vehicles, the severe effect of the proposed freeway control system can be seen when the No Control case is compared with the control algorithm applied cases, i.e., RM control using ALINEA, RM control using H_∞ SFC and combined RM + VSL control using H_∞ SFC. As can be seen from Fig. 5 to 8, the occupancies lower than 50% are maintainable for the located detectors during the simulation duration, even with a penetration rate of 0%. The increase in the penetration rate of vehicles with CACC has an uncertain effect on traffic flow

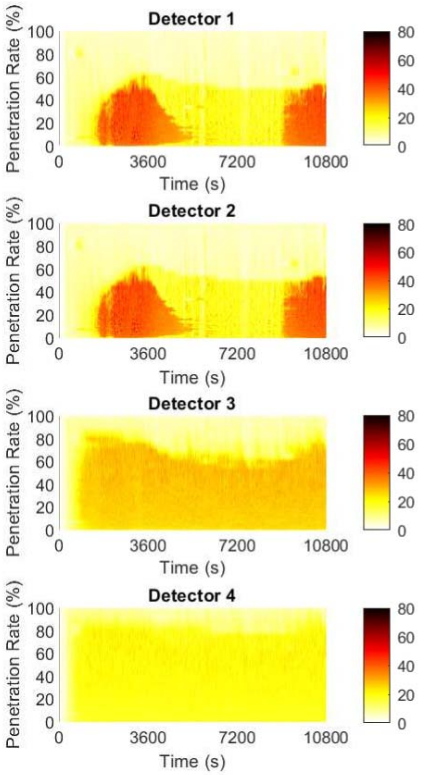

Fig. 7. Temporal variation of occupancies specific to penetration rates in only RM control case.

performance until it reaches to around 70-80%. From Fig. 5, it can be seen that in the case with a penetration rate less than 80 %, CACC is not sufficient to organize traffic flow

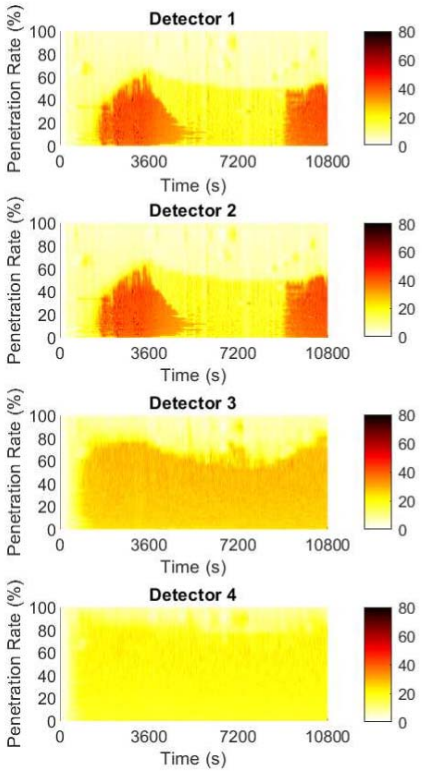

Fig. 8. Temporal variation of occupancies specific to penetration rates in combined control case involving coordinated RM and VSL.

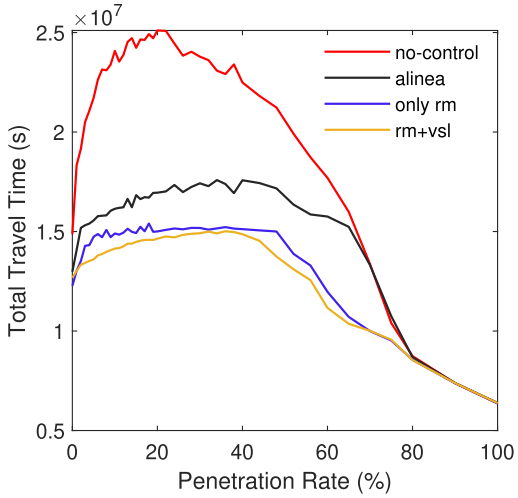

Fig. 9. Variation of total system travel time with respect to varying penetration rates specific to scenarios.

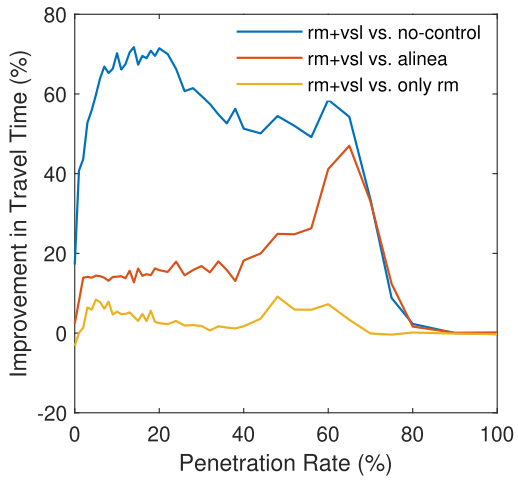

Fig. 10. Total system travel time improvement rates with respect to varying penetration rates specific to scenarios.

along a freeway with merging segments. From Fig. 5 to Fig. 8, the advantage of using the proposed system in comparison to ALINEA control can be clearly seen considering the results retrieved from Detector 1 and Detector 2. Under a 60% of penetration rate, the traffic congestion is mitigated faster with the control using the proposed system. In addition, using H_∞ SFC for RM control outperforms using ALINEA. Therefore, it is straightforward to conclude that the proposed algorithm reduces the duration of traffic congestion in a more effective way than ALINEA. Fig. 7 and Fig. 8 show that even if the proposed control strategy is not in V2I communication, it improves the traffic flow performance of the mainstream when compared to the corresponding penetration rate with no freeway control strategy. As the occupancies for the only-RM case and the combined RM + VSL case exist mostly under the same boundary in most of the time and penetration rate setups, a clear differentiation between the scenarios involving the occupancies cannot be made. Therefore, the total system travel time and the total system throughput are compared specific to scenarios as well. In Figs. 9 and 10, the total system travel times and total system travel time improvement rates retrieved from the simulation are presented with the variation of the penetration rate of vehicles with CACC.

As can be seen from Fig. 9, the increasing penetration rate does not improve the traffic flow performance until it reaches to around 50%. Although an increase in travel times has been expected due to the control delay from the control applied, decreases in the total system travel times have been observed in cases where the penetration rate of vehicles with CACC in traffic flow is under 50%, as a threshold. When this threshold is exceeded, the total system travel time for No Control case converges to the cases where control algorithms are employed, i.e., RM control using ALINEA, RM control using H_∞ SFC, and combined RM + VSL control using H_∞ SFC. In case of ALINEA use, a trend similar to other cases is observed regarding the relationship of penetration rate and total system travel time. However, at each penetration rate less than 80%, lower total system travel times are obtained in controlled cases using H_∞ SFC. Furthermore, it is seen that while the penetration rate of vehicles with CACC is higher than 80%, the proposed control strategies cannot provide any significant difference. In order to clearly figure out the performance of the combined RM + VSL system in terms of reductions in total system travel time, we have presented a comparison with the other cases, i.e., No Control, RM control using H_∞ SFC, and RM control using ALINEA. The positive impact of RM + VSL is remarkable for penetration rates less than 80%. For penetration rates in between 0 and 20%, the improvements increase

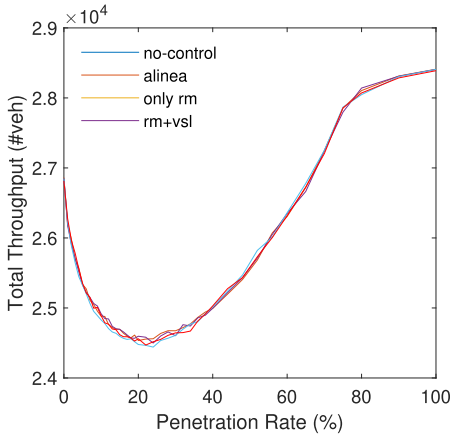

Fig. 11. Variation of total system throughput with respect to varying penetration rates specific to scenarios.

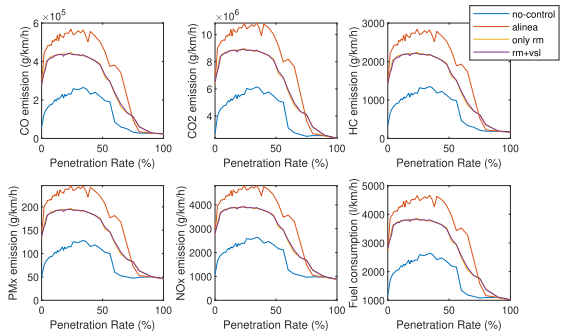

Fig. 12. Variation of pollutants emitted over on-ramps with respect to varying penetration rates.

to around 70%. Though the RM control using ALINEA is effective in reducing the total system travel time (see Fig. 9), the combined RM + VSL control using H_∞ SFC reduces total system travel time by more than 40% at a penetration rate of 60% when compared to ALINEA control. As the results obtained the controller we have designed for RM and combined RM + VSL cases are close to each other, the critical distinction among them can be seen in Fig. 10. In combined RM + VSL case, around 10% of reduction in total system travel time is obtained with penetration rates between 0 and 20%. Furthermore, at penetration rate of 40% to 60%, the combined RM + VSL control outperforms the only RM control by up to 10%. The total throughput of the system that corresponds to varying penetration rates for all the scenarios are presented in Fig. 11, where the decrease in the total throughput is clear until the penetration rate reaches to around 25%. Moreover, the initial value of the total system throughput cannot be attained, while the penetration rate is under 60%.

However, in cases with the penetration rate higher than 60%, the total throughput of the system has been increased by nearly 2000 vehicles per simulation with the selected vehicle attributes. In order to summarize our findings regarding the performance of the traffic flow throughout the case network using two control systems, i.e., the proposed integrated freeway control strategy and the CACC, the significance of three thresholds on the penetration rate of vehicles with CACC has to be highlighted. The first two threshold values are determined as 25% and 60% since the decrease in the performance of the traffic flow continues until the penetration rate reaches to 25%. Furthermore, when the penetration rate is increased to the third threshold that is 80%, the controls applied are not that effective since most of the performance measures considered converge to a single point for each of the scenarios.

To validate our findings on the performance of the traffic flow in terms of environmental measures obtained after applying the proposed control, a number of pollutants including the CO, CO_2, HC, PM_x, and NO_x, as well as the fuel consumption are considered. Considering the possibility that the number of idling vehicles in cases of merges could be increased due to the control applied, increases on the fuel consumption and the emissions have been expected. Therefore, the quantities of fuel consumption and emissions are retrieved separately, from the mainstream and the on-ramps, and then summed up to represent network-wide figures. As can be seen from Fig. 12, the emission quantities retrieved at on-ramps during the simulation of the No Control case are higher than that of the cases with control, which can be attributed to the fact that a control delay for each of the on-ramps is considered. However, one can expect that such an increase on the emissions from merging flows could be compensated by the decrease on the emissions from vehicles in the mainstream due to the control.

In our case, improvements obtained in terms of reduction on the total of emitted pollutants on the mainstream using the control system we have designed can be interpreted from Fig. 14, where the changes in emissions are compensated by the decreases from mainstream traffic. On one hand, as presented in Fig. 13, the increases in the total red time at on-ramps are consistent with the increases on emissions at on-ramps. On the other hand, the total travel time obtained specific to each controlled scenario is less than the No Control scenario, as shown in Fig. 9. Therefore, it is straightforward to conclude that increasing the control delay can be acceptable when the entire system is considered. It is important to note that in cases of varying traffic demands, such an interpretation may not be consistent, which requires case-specific simulations with different demand profiles in order to draw fair conclusions.

In Fig. 15, the totals of the pollutants emitted from the vehicles in the system throughout the network are shown. In order to validate our findings, we have analyzed the figures in terms of the thresholds regarding the penetration rate of CACC vehicles that are obtained through the performance analysis of the traffic flow. As can be seen from Fig. 12 to 15, a sharp increase on the total emitted pollutants lasts at the first threshold with 25%, and then the first decrease trend starts with a penetration rate of 50%. Regarding the second threshold determined, i.e., 60%, it can be said that the negative impact of the mixed traffic on flow is balanced. However, the third threshold determined, i.e., 80%, has not been satisfied for each of the pollutants and the fuel consumption. This is, first, due to the fact that the combined RM + VSL control of traffic with more than 80% of CACC vehicles has returned higher fuel consumptions and emissions when compared to No Control

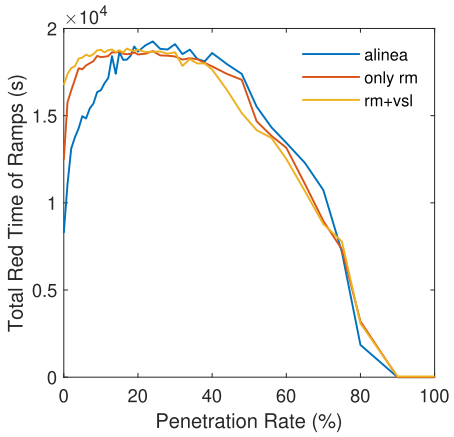

Fig. 13. Variation of total red times with respect to varying penetration rates.

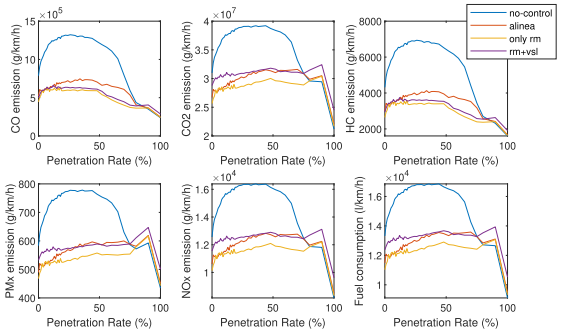

Fig. 14. Variation of pollutants emitted over mainstream with respect to varying penetration rates.

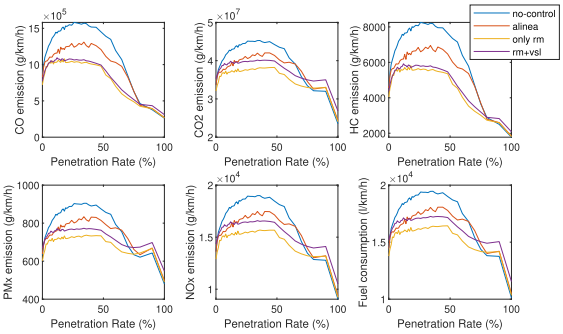

Fig. 15. Variation of pollutants emitted system-wide with respect to varying penetration rates.

and only RM control cases, which highlights the need to modify the control strategy according to the support of the CACC. Secondly, although being not in contrast to each other, findings involving the environmental measures and the traffic flow performances are not necessarily in parallel. Beyond the 80% threshold, the management of traffic flow is mostly provided through CACC, and hence, for improving the effectiveness of the controls we propose, the V2I communication is better to be incorporated.

Overall, the combined control we propose for the mixed traffic flow involving CAVs and HDVs returns system-wide effective results. It is important to note that the level of effectiveness is directly related to the penetration rate of vehicles with CACC. Therefore, it is straight to state that progressing and realizing freeway control strategies is highly dependent on projections on the increases of the penetration rate of CAVs.

VI. Conclusion

In this paper, we have presented in terms of flow dynamics and exhaust emissions the performance analysis of a novel H_∞ SFC based combined control we have designed involving coordinated RM and VSL and compared it with the well-known control algorithm ALINEA. The controller incorporated to the entire combined control strategy is tested considering mixed traffic that is composed of CAVs and HDVs, and the layout of a real-road network together with the actual flow measurements using the micro-simulation environment SUMO. It is important to note that in cases of varying traffic demands, such an interpretation may not be consistent, which requires case-specific simulations with different demand profiles in order to draw fair conclusions.

The results obtained have shown that the controller we propose in conjunction with the combined control is highly efficient in regulating the traffic density under a defined critical density, while tolerating the negative effects of lower levels of penetration rates smaller than 80% that possesses great importance in the introduction and early deployment of vehicles with CACC to freeway traffic. The results have shown as well that in cases with penetration rate of around 80%, the influence of the control applied fades away.

Our findings point out three critical levels of penetration rate for CACC equipped vehicles. Until the penetration rate reaches 25%, the mixed traffic has major negative impacts on the flow performance and the environment. Therefore, for the near-time deployment of CACC, some other ITS applications should be considered to reduce this adverse effect of CACC. Closer to the 60% of the penetration rate, the traffic flow performance reaches its initial performance. When 60% is exceeded, the improvements provided by the vehicles with CACC are at greatest, while around 80%, the traffic flow lose the need of being managed using ITS tools.

Future extensions of our study involve: improving the entire algorithm in order to increase its effectiveness in case of lower penetration rates; and, incorporating the cooperative lane-change and cooperative merging rules for both connected and conventional vehicles.

Appendix A
Proof of Theorem 1

Let us consider the Lyapunov function $V(\mathbf{x}) = \mathbf{x}^\top \mathbf{P}^{-1}\mathbf{x}$ and define $\Gamma(t) = \mathbf{x}^T(t)\mathbf{x}(t) - \gamma^2 \mathbf{w}^T(t)\mathbf{w}^T(t)$. Deriving V along the solutions of (19), we have

$$\dot{V}(t) + \Gamma(t) = 2\mathbf{x}^T(t)\mathbf{P}^{-1}\dot{\mathbf{x}}(t) + \mathbf{x}^T(t)\mathbf{x}(t) - \gamma^2 \mathbf{w}^T(t)\mathbf{w}^T(t)$$
$$= \begin{bmatrix}\mathbf{x}(t)\\ \mathbf{w}(t)\end{bmatrix}^T \begin{bmatrix}\overline{\Omega}_{11} + \mathbf{I} & \mathbf{P}^{-1}\mathbf{B}_\mathbf{w}\\ * & -\gamma^2\mathbf{I}\end{bmatrix}\begin{bmatrix}\mathbf{x}(t)\\ \mathbf{w}(t)\end{bmatrix}$$

where $\overline{\Omega}_{11} = \mathbf{A_K}^T\mathbf{P}^{-1} + \mathbf{P}^{-1}\mathbf{A_K}$. By state transformation, one can write

$$\dot{V}(t) + \Gamma(t) = \begin{bmatrix} \mathbf{x}(t) \\ \mathbf{w}(t) \end{bmatrix}^T \begin{bmatrix} \mathbf{P}^{-1} \\ \mathbf{I} \end{bmatrix}^T \begin{bmatrix} \Omega_{11} + \mathbf{P}^T\mathbf{P} & \mathbf{B_w} \\ * & -\gamma^2\mathbf{I} \end{bmatrix} \times \begin{bmatrix} \mathbf{P}^{-1} \\ \mathbf{I} \end{bmatrix} \begin{bmatrix} \mathbf{x}(t) \\ \mathbf{w}(t) \end{bmatrix}.$$

By using Schur complement and (20), we obtain

$$\dot{V}(t) + \Gamma(t) < 0. \tag{32}$$

For $\mathbf{w}(t) = 0$, for all $t \geq 0$, (32) implies that

$$\dot{V}(t) < 0.$$

Moreover, replacing $\Gamma(t)$ into (32) yields

$$\dot{V}(t) < \gamma^2\mathbf{w}^T(t)\mathbf{w}^T(t) - \mathbf{x}^T(t)\mathbf{x}(t),$$

which completes the proof.

REFERENCES

[1] P. Kachroo and K. Ozbay, *Feedback Ramp Metering in Intelligent Transportation Systems*. New York, NY, USA: Kluwer, 2003.

[2] H. Haj-Salem and M. Papageorgiou, "Ramp metering impact on urban corridor traffic: Field results," *Transp. Res. A, Policy Pract.*, vol. 29, no. 4, pp. 303–319, Jul. 1995.

[3] H. Zhang, S. G. Ritchie, and W. W. Recker, "Some general results on the optimal ramp control problem," *Transp. Res. C, Emerg. Technol.*, vol. 4, no. 2, pp. 51–69, Apr. 1996.

[4] H. M. Zhang and S. G. Ritchie, "Freeway ramp metering using artificial neural networks," *Transp. Res. C, Emerg. Technol.*, vol. 5, no. 5, pp. 273–286, Oct. 1997.

[5] H. M. Zhang, S. G. Ritchie, and R. Jayakrishnan, "Coordinated traffic-responsive ramp control via nonlinear state feedback," *Transp. Res. C, Emerg. Technol.*, vol. 9, no. 5, pp. 337–352, Oct. 2001.

[6] E. Smaragdis, M. Papageorgiou, and E. Kosmatopoulos, "A flow-maximizing adaptive local ramp metering strategy," *Transp. Res. B, Methodol.*, vol. 38, no. 3, pp. 251–270, Mar. 2004.

[7] M. J. Cassidy and J. Rudjanakanoknad, "Increasing the capacity of an isolated merge by metering its on-ramp," *Transp. Res. B, Methodol.*, vol. 39, no. 10, pp. 896–913, 2005.

[8] G. Gomes and R. Horowitz, "Optimal freeway ramp metering using the asymmetric cell transmission model," *Transp. Res. C, Emerg. Technol.*, vol. 14, no. 4, pp. 244–262, 2006.

[9] Z. S. Hou, J.-X. Xu, and J. W. Yan, "An iterative learning approach for density control of freeway traffic flow via ramp metering," *Transp. Res. C, Emerg. Technol.*, vol. 16, no. 1, pp. 71–97, Feb. 2008.

[10] G. Gomes, R. Horowitz, A. A. Kurzhanskiy, P. Varaiya, and J. Kwon, "Behavior of the cell transmission model and effectiveness of ramp metering," *Transp. Res. C, Emerg. Technol.*, vol. 16, no. 4, pp. 485–513, 2008.

[11] I. Papamichail, A. Kotsialos, I. Margonis, and M. Papageorgiou, "Coordinated ramp metering for freeway networks—A model-predictive hierarchical control approach," *Transp. Res. C, Emerg. Technol.*, vol. 18, pp. 311–331, Jun. 2010.

[12] J. Haddad, M. Ramezani, and N. Geroliminis, "Cooperative traffic control of a mixed network with two urban regions and a freeway," *Transp. Res. B, Methodol.*, vol. 54, no. 8, pp. 17–36, Aug. 2013.

[13] C. Pasquale, I. Papamichail, C. Roncoli, S. Sacone, S. Siri, and M. Papageorgiou, "Two-class freeway traffic regulation to reduce congestion and emissions via nonlinear optimal control," *Transp. Res. C, Emerg. Technol.*, vol. 55, pp. 85–99, Jun. 2015.

[14] Y. Kan, Y. Wang, M. Papageorgiou, and I. Papamichail, "Local ramp metering with distant downstream bottlenecks: A comparative study," *Transp. Res. C, Emerg. Technol.*, vol. 62, pp. 149–170, Jan. 2016.

[15] F. Soriguera, I. Martínez, M. Sala, and M. Menéndez, "Effects of low speed limits on freeway traffic flow," *Transp. Res. C, Emerg. Technol.*, vol. 77, pp. 257–274, Apr. 2017.

[16] M. Papageorgiou, "An integrated control approach for traffic corridors," *Transp. Res. C, Emerg. Technol.*, vol. 3, no. 1, pp. 19–30, 1995.

[17] A. Kotsialos, M. Papageorgiou, M. Mangeas, and H. Haj-Salem, "Coordinated and integrated control of motorway networks via non-linear optimal control," *Transp. Res. C, Emerg. Technol.*, vol. 10, no. 1, pp. 65–84, Feb. 2002.

[18] C. Pasquale, S. Sacone, S. Siri, and B. De Schutter, "A multi-class model-based control scheme for reducing congestion and emissions in freeway networks by combining ramp metering and route guidance," *Transp. Res. C, Emerg. Technol.*, vol. 80, pp. 384–408, Jul. 2017.

[19] Y. Zhang and P. A. Ioannou, "Coordinated variable speed limit, ramp metering and lane change control of highway traffic," *IFAC-PapersOnLine*, vol. 50, no. 1, pp. 5307–5312, Jul. 2017.

[20] A. Hegyi, B. De Schutter, and J. Hellendoorn, "Model predictive control for optimal coordination of ramp metering and variable speed limits," *Transp. Res. C, Emerg. Technol.*, vol. 13, no. 3, pp. 185–209, Jun. 2005.

[21] R. C. Carlson, I. P. M. Papamichail, and A. Messmer, "Optimal mainstream traffic flow control of large-scale motorway networks," *Transp. Res. C, Emerg. Technol.*, vol. 18, no. 2, pp. 193–212, 2010.

[22] J. R. D. Frejo and E. F. Camacho, "Global versus local MPC algorithms in freeway traffic control with ramp metering and variable speed limits," *IEEE Trans. Intell. Transp. Syst.*, vol. 13, no. 4, pp. 1556–1565, Dec. 2012.

[23] R. C. Carlson, I. Papamichail, and M. Papageorgiou, "Integrated feedback ramp metering and mainstream traffic flow control on motorways using variable speed limits," *Transp. Res. C, Emerg. Technol.*, vol. 46, pp. 209–221, Sep. 2014.

[24] J. R. D. Frejo, A. Núñez, B. De Schutter, and E. F. Camacho, "Hybrid model predictive control for freeway traffic using discrete speed limit signals," *Transp. Res. Part C, Emerg. Technol.*, vol. 46, pp. 309–325, Sep. 2014.

[25] C. Roncoli, M. Papageorgiou, and I. Papamichail, "Traffic flow optimisation in presence of vehicle automation and communication systems—Part II: Optimal control for multi-lane motorways," *Transp. Res. C, Emerg. Technol.*, vol. 57, pp. 260–275, Aug. 2015.

[26] C. Roncoli, I. Papamichail, and M. Papageorgiou, "Hierarchical model predictive control for multi-lane motorways in presence of vehicle automation and communication systems," *Transp. Res. C, Emerg. Technol.*, vol. 62, pp. 117–132, Jan. 2016.

[27] P. A. Ioannou and C. C. Chien, "Autonomous intelligent cruise control," *IEEE Trans. Veh. Technol.*, vol. 42, no. 4, pp. 657–672, Nov. 1993.

[28] M. Wang, M. Treiber, W. Daamen, S. P. Hoogendoorn, and B. van Arem, "Modelling supported driving as an optimal control cycle: Framework and model characteristics," *Transp. Res. C, Emerg. Technol.*, vol. 36, pp. 547–563, Nov. 2013.

[29] B. HomChaudhuri, A. Vahidi, and P. Pisu, "A fuel economic model predictive control strategy for a group of connected vehicles in urban roads," in *Proc. Amer. Control Conf. (ACC)*, Jul. 2015, pp. 2741–2746.

[30] Y. Zhou, S. Ahn, M. Chitturi, and D. A. Noyce, "Rolling horizon stochastic optimal control strategy for ACC and CACC under uncertainty," *Transp. Res. C, Emerg. Technol.*, vol. 83, pp. 61–76, Oct. 2017.

[31] V. Milanés and S. E. Shladover, "Modeling cooperative and autonomous adaptive cruise control dynamic responses using experimental data," *Transp. Res. C, Emerg. Technol.*, vol. 48, pp. 285–300, Nov. 2014.

[32] D. Li, Y. Zhao, P. Ranjitkar, H. Zhao, and Q. Bai, "Hybrid approach for variable speed limit implementation and application to mixed traffic conditions with connected autonomous vehicles," *IET Intell. Transp. Syst.*, vol. 12, no. 5, pp. 327–334, Jun. 2018.

[33] A. Talebpour and H. S. Mahmassani, "Influence of connected and autonomous vehicles on traffic flow stability and throughput," *Transp. Res. C, Emerg. Technol.*, vol. 71, pp. 143–163, Oct. 2016.

[34] S. Lee, B. G. Heydecker, J. Kim, and S. Park, "Stability analysis on a dynamical model of route choice in a connected vehicle environment," *Transp. Res. Procedia*, vol. 23, pp. 720–737, Jan. 2017.

[35] L. Xiao, M. Wang, W. Schakel, and B. van Arem, "Unravelling effects of cooperative adaptive cruise control deactivation on traffic flow characteristics at merging bottlenecks," *Transp. Res. C, Emerg. Technol.*, vol. 96, pp. 380–397, Nov. 2018.

[36] Y. Tu, W. Wang, Y. Li, C. Xu, T. Xu, and X. Li, "Longitudinal safety impacts of cooperative adaptive cruise control vehicle's degradation," *J. Saf. Res.*, vol. 69, pp. 177–192, Jun. 2019.

[37] Y. Li, C. Xu, L. Xing, and W. Wang, "Integrated cooperative adaptive cruise and variable speed limit controls for reducing rear-end collision risks near freeway bottlenecks based on micro-simulations," *IEEE Trans. Intell. Transp. Syst.*, vol. 18, no. 11, pp. 3157–3167, Nov. 2017.

[38] Y. Li, H. Wang, W. Wang, L. Xing, S. Liu, and X. Wei, "Evaluation of the impacts of cooperative adaptive cruise control on reducing rear-end collision risks on freeways," *Accident Anal. Prevention*, vol. 98, pp. 87–95, Jan. 2017.
[39] B. van Arem, C. J. G. van Driel, and R. Visser, "The impact of cooperative adaptive cruise control on traffic-flow characteristics," *IEEE Trans. Intell. Transp. Syst.*, vol. 7, no. 4, pp. 429–436, Dec. 2006.
[40] L. Zhao and J. Sun, "Simulation framework for vehicle platooning and car-following behaviors under connected-vehicle environment," *Procedia-Social Behav. Sci.*, vol. 96, pp. 914–924, Nov. 2013.
[41] F. Knorr, D. Baselt, M. Schreckenberg, and M. Mauve, "Reducing traffic jams via VANETs," *IEEE Trans. Veh. Technol.*, vol. 61, no. 8, pp. 3490–3498, Oct. 2012.
[42] A. I. Delis, I. K. Nikolos, and M. Papageorgiou, "Simulation of the penetration rate effects of ACC and CACC on macroscopic traffic dynamics," in *Proc. IEEE 19th Int. Conf. Intell. Transp. Syst. (ITSC)*, Nov. 2016, pp. 336–341.
[43] H. Liu, X. Kan, S. E. Shladover, X. Y. Lu, and R. E. Ferlis, "Modeling impacts of cooperative adaptive cruise control on mixed traffic flow in multi-lane freeway facilities," *Transp. Res. C, Emerg. Technol.*, vol. 95, pp. 261–279, Oct. 2018.
[44] C. Dym, *Principles of Mathematical Modeling*. Amsterdam, The Netherlands: Elsevier, 2004.
[45] M. Treiber, A. Hennecke, and D. Helbing, "Congested traffic states in empirical observations and microscopic simulations," *Phys. Rev. E, Stat. Phys. Plasmas Fluids Relat. Interdiscip. Top.*, vol. 62, no. 2, p. 1805, 2000.
[46] K. E. Wunderlich, M. Vasudevan, and P. Wang, "Traffic analysis toolbox volume III: Guidelines for applying traffic microsimulation modeling software 2019 update to the 2004 version," Federal Highway Admin., Washington, DC, USA, Tech. Rep. FHWA-HOP-18-036, 2019.
[47] T. V. Woensel and N. Vandaele, "Empirical validation of a queueing approach to uninterrupted traffic flows," *4OR*, vol. 4, no. 1, pp. 59–72, Mar. 2006.
[48] J. Barcelo *et al.*, *Fundamentals of Traffic Simulation*, vol. 145. Springer, 2010.
[49] M. Lindorfer, C. F. Mecklenbräuker, and G. Ostermayer, "Modeling the imperfect driver: Incorporating human factors in a microscopic traffic model," *IEEE Trans. Intell. Transp. Syst.*, vol. 19, no. 9, pp. 2856–2870, Sep. 2018.
[50] L. Xiao, M. Wang, and B. van Arem, "Realistic car-following models for microscopic simulation of adaptive and cooperative adaptive cruise control vehicles," *Transp. Res. Rec.*, vol. 2623, no. 1, pp. 1–9, Jan. 2017.
[51] J. Erdmann, "Lane-changing model in sumo," in *Modeling Mobility With Open Data*, vol. 24. Berlin, Germany: Deutsches Zentrum für Luft- und Raumfahrt, 2014, pp. 77–88.

Mehmet Ali Silgu (Member, IEEE) was born in Istanbul, Turkey, in 1988. He received the M.Sc. degree in transportation engineering from the Technical University of Istanbul (ITU) in 2015, where he is currently pursuing the Ph.D. degree.

İsmet Gökşad Erdağı (Member, IEEE) was born in Kars, Turkey, in 1994. He received the B.Sc. degree in civil engineering from the Technical University of Istanbul in 2018, where he is currently pursuing the M.Sc. degree in transportation engineering.

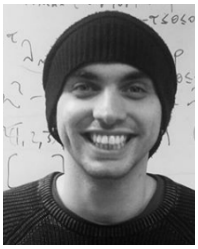

Gökhan Göksu was born in Istanbul, Turkey, in 1988. He received the B.Sc. degree in mathematical engineering (major), the B.Sc. degree in physics engineering (minor), the M.Sc. degree in transportation engineering, and the Ph.D. degree in mathematical engineering from Istanbul Technical University (ITU), in 2011, 2015, 2013, and 2020, respectively. From February 2019 to April 2020, he was a Researcher with the Laboratoire des Signaux et Systèmes (L2S), CentraleSupélec, Université Paris-Saclay. He is currently a Post-Doctoral Scholar with the ITU ITS Research Laboratory.

Hilmi Berk Celikoglu (Senior Member, IEEE) was born in Istanbul, Turkey, in 1976. He received the B.S., M.S., and Ph.D. degrees from Istanbul Technical University (ITU), Istanbul, in 2000, 2002, and 2006, respectively. He has been a Full Professor, specialized in traffic flow theories and transportation network modeling, with the Department of Civil Engineering, ITU, and the Director of the ITU ITS Research Laboratory since 2014. He was a Visiting Professor with the Department of Computer Science and Mathematics, Penn State Harrisburg, from 2014 to 2015. He has been on the Editorial Board of the *Transportation Research Part C: Emerging Technologies*. He is an Associate Editor of the IEEE TRANSACTIONS ON INTELLIGENT TRANSPORTATION SYSTEMS and *IEEE Intelligent Transportation Systems Magazine*.